A subband calculation for the $SrTiO_3$/Nb:$SrTiO_3$/$SrTiO_3$ heterostructure

Introduction

We show the results of numerical calculations of the subband structure for the $SrTiO_3$/Nb:$SrTiO_3$/$SrTiO_3$ heterostructure. We first solve Poisson's equation to calculate the potential profile, and then derive the eigenstate energies E_n and envelope wavefunctions ψ_n (n is the quantum number for each eigenstate) for the potential by solving Schrödinger's equation[S1]. Both equations are solved using a conventional Runge-Kutta method. The assumptions are the following:

- 5.5 nm-thick 1 at. % Nb-doped $SrTiO_3$ layer is embedded in undoped $SrTiO_3$ layers.
- All dopants are fully activated.
- The potential is symmetric with respect to the centre of the Nb-doped $SrTiO_3$ layer.

There are two further points to be considered in the case of $SrTiO_3$. One is the permittivity of $SrTiO_3$, which is strongly dependent on the electric field. This can drastically modify the potential profile, as we demonstrate below. The relative permittivity is empirically expressed as[S2]

$$\varepsilon(F) = 1 + \frac{b}{\sqrt{a + F^2}}, \tag{S1}$$

where F is the electric field, $a = 2.79 \times 10^9$ V^2/m^2 and $b = 1.37 \times 10^9$ V/m are constants at low temperature. The second key feature is the conduction band structure, which is composed of heavy, light (and tetragonally split) and spin-orbit split bands[S3]. To investigate these effects, we carried out calculations in the following three cases:

1. A single parabolic band is used with the experimentally determined effective mass m^* of $1.24m_0$, for a potential assuming constant (zero field) permittivity. (Fig. S1)
2. A single parabolic band is used with the experimentally determined $m^* = 1.24m_0$, for a potential including the electric field dependent permittivity at the level of approximation in Ref. S2. (Fig. S2)
3. Three parabolic bands are used for the potential derived using the electric field dependent permittivity. (Fig. S3)

In the final case we used effective masses along the (100) direction at the Γ point of $1.9m_0$, $1.14m_0$ and $1.43m_0$ for the heavy ($E^{(1)}$), light and tetragonally split ($E^{(2)}$) and spin-orbit split ($E^{(3)}$) bands, respectively. The tetragonal splitting was $\Delta_t = 1.54$ meV and the spin-orbit splitting was $\Delta_{so} = 18$ meV. These values were taken from Ref. S4 for bulk $SrTiO_3$, which we simply assumed to be intact under two-dimensional confinement. Here we take the local dielectric approximation, and assume no inter-subband coupling.

Results and discussions

Figure S1 shows the result of Case 1, where a constant permittivity and a single band are assumed. Because $\varepsilon(0)$ exceeds 20,000 the confining potential is quite weak. Accordingly, the spacing between eigenstate energies is rather small, leading to a large number of occupied subbands. The Fermi energy E_F was determined self-consistently by insuring that the total electron density corresponds to the total number of dopants. By summing up the electron densities of each subband, the local 3D electron density N_{3D} is calculated as a function of position x and is also plotted. The electron distribution extends to $x \sim 24$ nm if we take the half-maximum (x_{hm}) value, and $x \sim 40$ nm if we take the threshold below which 90% of the electrons are accounted for ($x_{90\%}$), both of which are much larger than the range of dopants ($|x| < 2.75$ nm). These measures of the electron width are also far wider than the superconducting thickness determined from the upper critical field anisotropy (8.4 nm, corresponding to $x_{SC} = 4.2$ nm), and thus corresponds very poorly to the data.

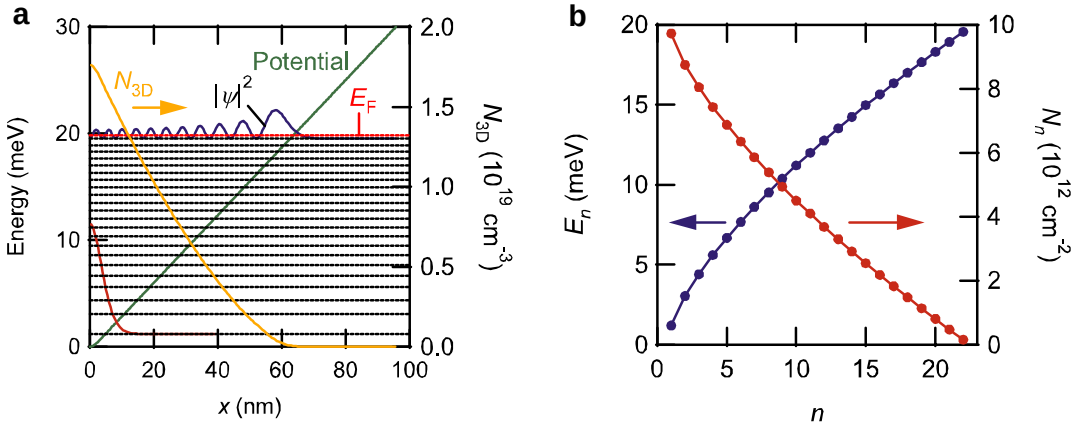

Figure S1 | Result of subband calculations for Case 1 (single band, linear dielectric). **a**, Potential profile, eigenstate energies, local electron density N_{3D} and corresponding envelope wavefunctions for the case of constant $\varepsilon = \varepsilon(0)$ and a single band with $m^* = 1.24m_0$. The wavefunctions are arbitrarily scaled and shifted upward by E_n. Only two wavefunctions with the lowest and highest energies are shown. **b**, Eigenstate energy and carrier density for each subband as a function of the quantum number n.

Figure S2 shows the calculation for Case 2, where the inclusion of the ε nonlinearity leads to a strong modification of the potential profile. The suppression of ε by the electric field gives a much narrower and more confining potential well, leading to a larger spacing between the eigenstate energies, and hence a smaller number of occupied subbands. In this case x_{hm} is 4.3 nm and $x_{90\%}$ is 5.0 nm, corresponding reasonably well with the experimentally determined x_{SC} = 4.2 nm. Here the range of local electron density is consistent with the bulk superconducting phase diagram[S5], and $x_{90\%}$ is approximately the 3D density threshold for the onset of bulk superconductivity.

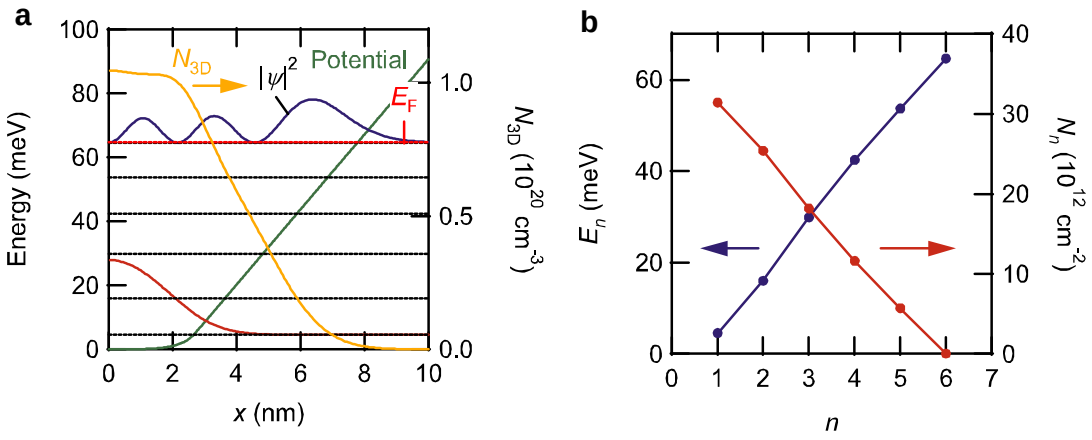

Figure S2 | Result of subband calculations for Case 2 (single band, nonlinear dielectric). a, Potential profile, eigenstate energies, local electron density N_{3D} and corresponding envelope wavefunctions for the case of electric-field dependent ε and a single band with $m^* = 1.24m_0$. The wavefunctions are arbitrarily scaled and shifted upward by E_n. Only two wavefunctions with the lowest and highest energies are shown. **b**, Eigenstate energy and carrier density for each subband.

Finally, in Case 3, we consider the effects of three nondegenerate conduction bands of $SrTiO_3$ using the bulk parameters given above, as well as dielectric nonlinearities, the results of which are shown in Fig. S3. Now x_{hm} is ~ 3.3 nm and $x_{90\%}$ is 3.6 nm, again in reasonable agreement with the experimental value. Case 3 is likely to be the best approximation to the actual electronic configuration, at this level of calculation. Here E_F is 35 meV. Using this value, the Fermi velocity $v_F = 8.1 \times 10^6$ cm/s is determined for the lowest heavy electron subband, corresponding to a mean free path $l_{mfp} = v_F \tau = 97$ nm. In

the case that the Shubnikov-de Haas oscillations we have observed correspond to the three light electron subbands, the corresponding values for the lowest light electron subband are $v_F = 1.0 \times 10^7$ cm/s and $l_{mfp} = 74$ nm.

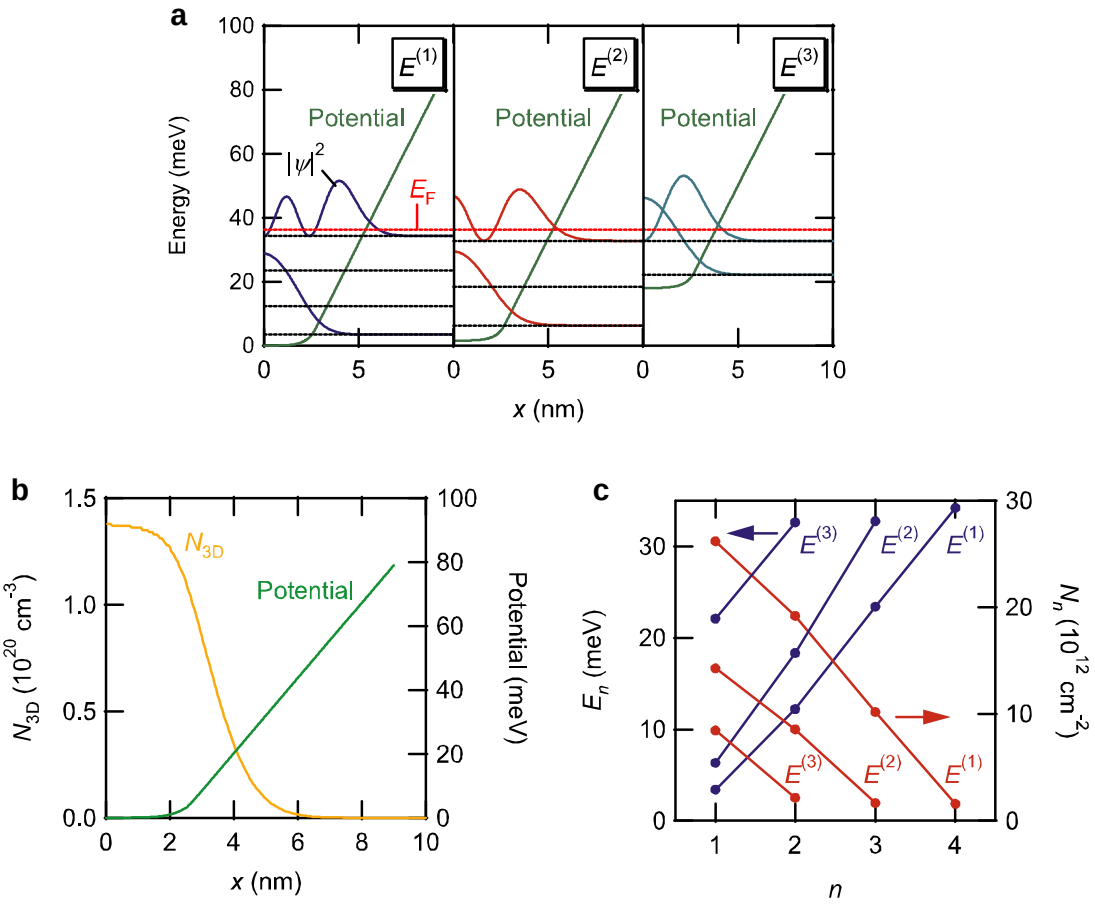

Figure S3 | Result of subband calculations for Case 3 (three bulk-like bands, nonlinear dielectric). a, Potential profile and eigenstate energies for the case of three conduction bands (bulk values) with an electric-field dependent ε. The potential, envelope wavefunctions and eigenstate energies are shifted by the corresponding energies $\Delta_t = 1.54$ meV and $\Delta_{so} = 18$ meV for the tetragonally split light electron band $E^{(2)}$ and spin-orbit split band $E^{(3)}$. **b,** Local electron density N_{3D} and potential versus position. **c,** Eigenstate energy and carrier density are plotted as a function of n for each conduction subband.

Limitations

In these calculations, a number of simplifying approximations have been made, which include the following:

- Full electrostatic self-consistency of the fixed-charge potential with the electron distribution was not considered. Particularly with a strong dielectric nonlinearity, this may induce nontrivial corrections beyond those observed in conventional semiconductors.
- $d\varepsilon/dx$ (i.e. polarization charge) and nonlocal dielectric effects were not incorporated, both of which grow in importance for large short-length-scale variations in the potential.
- The electron pocket structure of bulk $SrTiO_3$ has been shown theoretically to be sensitive to both the tetragonal distortion and TiO_6 octahedral rotation[S3], which has not been considered here by using only fixed bulk values. The deviation of the potential in Figs. S2 and S3 from a simple triangular well can be considered a proxy for spatial variations in the local crystal structure. When incorporated, the local electronic structure will also vary spatially.

In light of these simplifications, the calculations presented here should be considered to be a rough guide. A detailed numerical comparison would require a much more sophisticated calculation addressing these points.

References:

S1. *Delta-doping of semiconductors*, edited by Schubert, E. F. (Cambridge University Press, Cambridge, 1996).

S2. Yamamoto, T., Suzuki, S., Kawaguchi, K. & Takahashi, K. Temperature dependence of the ideality factor of $Ba_{1-x}K_xBiO_3$/Nb-doped $SrTiO_3$ all-oxide-type Schottky junctions. *Jpn. J. Appl. Phys.* **37**, 4737-4746 (1998).

S3. Mattheiss, L. F. Effect of the 110°K phase transition on the $SrTiO_3$ conduction bands. *Phys. Rev. B* **6,** 4740-4753 (1972).

S4. Uwe, H., Sakudo, T. & Yamaguchi, H. Interband electronic Raman scattering in $SrTiO_3$. *Jpn. J. Appl. Phys.* **24,** suppl. 24-2, 519-521 (1985).

S5. Koonce, C. S., Cohen, M. L., Schooley, J. F., Hosler, W. R. & Pfeiffer, E. R. Superconducting transition temperatures of semiconducting $SrTiO_3$. *Phys. Rev.* **163**, 380-390 (1967).